Tank Treading and Unbinding of Deformable Vesicles in Shear Flow: Determination of the Lift Force

Manouk Abkarian, Colette Lartigue, and Annie Viallat*

Laboratoire de Spectrométrie Physique, UMR C5588 (CNRS); Université Joseph Fourier BP87 38402 Saint Martin d'Hères Cedex, France

(Received 24 July 2001; published 25 January 2002)

Deformation and tank-treading motion of flaccid vesicles in a linear shear flow close to a wall are quantitatively studied by light microscopy. Velocities of bounded vesicles obey Goldman's law established for rigid spheres. A progressive tilt and a transition of unbinding of vesicles are evidenced upon increasing the shear rate, $\dot{\gamma}$. These observations disclose the existence of a viscous lift force, F_l, depending on the viscosity η of the fluid, the radius R of the vesicle, its distance h from the substrate, and a monotonous decreasing function $f(1-v)$ of the reduced volume v, in the following manner: $F_l = \eta\dot{\gamma}(R^3/h)f(1-v)$. This relation is valid for vesicles both close to and farther from the substrate.

DOI: 10.1103/PhysRevLett.88.068103 PACS numbers: 87.16.Dg, 47.15.Gf, 87.19.St

A lipid vesicle is a closed, fluid and water-permeable membrane filled by an aqueous solution. A number of theoretical works have recently attempted to predict the behavior of weakly adhesive vesicles in a bounded shear flow [1–4]. This problem is far from trivial due to the ability of flaccid vesicles to undergo flow-induced deformations (free-interface problem). Indeed, vesicle shapes are not given *a priori*. They are governed by the hydrodynamic forces, the internal fluid viscosity, the bending elasticity, and the constraints of fixed volume and area (nonextensibility of the membrane). For instance, the behavior of vesicles in shear flow differs from that of liquid droplets, whose area can vary and whose shape is governed by the surface tension [5]. Rheological properties of vesicles are at the origin of two types of motion predicted under flow: the flipping expected when the contrast of viscosity between the inner and the outer fluid is high (red blood cells), and the tank-treading motion with fixed vesicle orientation predicted for low viscosity contrast [4,6]. In this latter situation, theories predict that vesicles are asymmetric and experience a lift force, which can lead to their unbinding from the substrate [1,2]. The quantitative determination of this lift force appears as a basic stage on the way to understanding the behavior of erythrocytes and leukocytes in the blood flow, where they are subjected to strong shear forces. This lift force may play a significant role in the early stage of the inflammatory response, when a leukocyte leaves the blood flow to adhere and roll onto the endothelium [7,8]. However, the law of variation of the lift force with its driving parameters has not been established up to now, due to a lack of fast 3D-numerical approaches and of extensive experiments. Recently, unbinding of one weakly adhesive vesicle in a shear flow has been reported without detecting any shape deformation [9].

In this Letter, we describe in detail the behavior of nonadhesive settled flaccid vesicles in a shear flow close to a wall. By direct side-view observation, we describe quantitatively and we interpret vesicle motion: unbinding, tank treading, and sliding. This allows us to reveal and to determine the lift force for which we propose a law of variation, relying, for the first time to our knowledge, on a complete set of experiments.

Giant phospholipidic vesicles were swollen from L-α dioleyol-phosphatidylcholine using the electroformation method [10]. They were prepared in sucrose solutions of various concentrations (50, 100, 200, and 250 mM) and diluted in glucose solutions (50–290 mM) of higher osmolalities during at least one hour in order to slightly deswell the vesicles. However, at the scale of a few minutes (typically the time of a flow experiment), vesicle membranes can be considered as impermeable. All solutions were made at $p\mathrm{H} = 7.4$. The flow was applied using a syringe pump in a parallelepiped flow chamber with four optical faces ($1 \times 10 \times 45$ mm). The laminar shear rate was calibrated using suspensions of 2 μm diameter latex beads. Tipping the microscope at 90° and working at low-angle incidence allowed us to observe well-defined side-view images of both vesicles and their reflections on the substrate. Image analysis was performed using an image software (NIH, 1.62c).

Vesicles were gently injected into the chamber, allowed to settle, and observed at rest. A shear flow was then applied in the chamber. The shear rate was slowly increased step by step, so that vesicles reached a constant velocity during each step. At the end of the experiment, the flow was stopped and we checked that the vesicles retrieved their initial shape.

A typical experiment is illustrated in Fig. 1 for one vesicle. At rest, it is deflated and axisymmetric [Fig. 1(a)]. It undergoes a shape deformation when a shear rate $\dot{\gamma}$ is applied: its fore-aft symmetry is lost and a progressive tilt is observed. The vesicle slowly moves along the flow direction, keeping a stationary shape and a fixed orientation [Fig. 1(b)]. When the shear rate progressively increases above a value $\dot{\gamma}_c$, the vesicle unbinds [Fig. 1(c)] and moves away from the substrate Figs. 1(d) and 1(e), while its shape tends to a prolate ellipsoid [11].

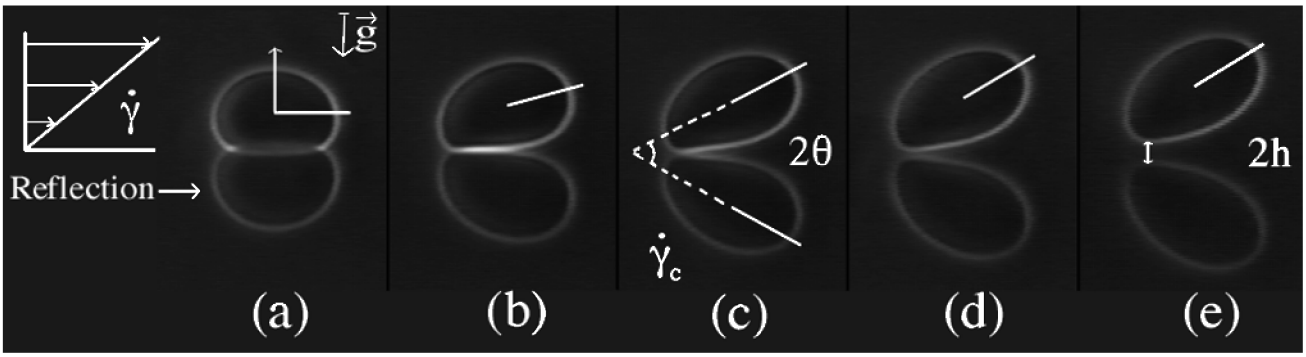

FIG. 1. Side-view image of a vesicle ($R = 31$ μm, reduced volume $v = 0.94$, weight $P = 16$ pN). The lowest image is the reflection on the substrate: (a) at rest, (b) at shear rate $\dot{\gamma}$ equal to 0.4 s^{-1}, (c) 0.9 s^{-1}, (d) 1.1 s^{-1}, and (e) 2.5 s^{-1}. The white line is the direction of the longest axis of inertia.

It is noteworthy that all quasispherical vesicles were not deformed by the flow and remained settled on the substrate under large shear rate, up to $\dot{\gamma} = 8$ s^{-1}.

Shape analysis and orientations.—The enclosed volume $\mathcal{V}$ and the surface area S of each vesicle were determined from their contour at rest by a method of azimuthal integration [12]. We characterized each vesicle by its effective radius, defined as $R = (3\mathcal{V}/4\pi)^{1/3}$, and its reduced volume (dimensionless number), $v = \mathcal{V}/[\frac{4}{3}\pi(\frac{S}{4\pi})^{3/2}]$, which measures its state of deswelling ($v = 1$ for a sphere). Vesicle deformability increases with $(1 - v)$. The integration method gave the position of the vesicle center of mass during the motion. It also yielded the direction of its two principal axes of inertia, the angle θ of inclination of the longest axis of the vesicle with respect to the flow direction, and the vesicle-substrate distance h. When the shear rate increases up to $\dot{\gamma}_c$, the inclination angle θ increases rapidly. At $\dot{\gamma}_c$, the value of the tilt θ is very close to a limiting value θ_l, which is reached when the wall-vesicle distance is of the order of magnitude of one vesicle radius. The value of θ_l depends only on the reduced volume v. This result can be understood by considering that the vesicles experience torques due to the shear flow and to the tank-treading motion. The balance of these two torques, both proportional to $\dot{\gamma}$, results in a steady tilt independent of the shear rate. Variation of θ_l with v is in good agreement with theoretical predictions [13] and observations [14] concerning vesicles in nonbounded shear flow. The vesicle shape is therefore not affected by the wall at distances larger than approximately one radius.

Sliding and tank treading.—Vesicle tank treading was clearly observed from the rotational motion of one defect linked to the membrane. This motion allowed us to measure the membrane angular velocity ω for two vesicles. We also measured the translational velocity V of the center of mass along the flow direction for all studied vesicles. Variations of V and ωR versus the shear rate $\dot{\gamma}$ are linear as long as the vesicles remain bounded to the substrate (Fig. 2). The ratio $\omega R/V$ was found equal to 0.49 and 0.51 for two vesicles of radii 14.8 and 18 μm, respectively. These values show that vesicles roll and slide along the wall in the same proportion. A combination of sliding and rolling has been previously reported on vesicles moving close to a wall under gravity [15].

In order to further explore the laws of vesicle motion, we plotted the variations of the ratio $V/\dot{\gamma}$ versus R for all studied vesicles (Fig. 3). The data fall on a single curve independent on the reduced volume of the vesicles: data obtained on quasispherical nondeformable vesicles lie on the curve together with that on deflated vesicles. This feature corroborates recent 2D-numerical simulations [16], which show that the dominant term of the hydrodynamic dissipation in the motion of moderately deflated vesicles, deviates less than 5% from that of a sphere. These results led us to use the Goldman model proposed for the motion of rigid spheres [17], in the limit $h_0/R \ll 1$, where h_0 is the distance between the surface of the sphere and the substrate. The model yields

$$\frac{V}{\dot{\gamma}} = \frac{(R + h_0)}{0.8580 - 0.2691 \ln(\frac{h_0}{R})}. \qquad (1)$$

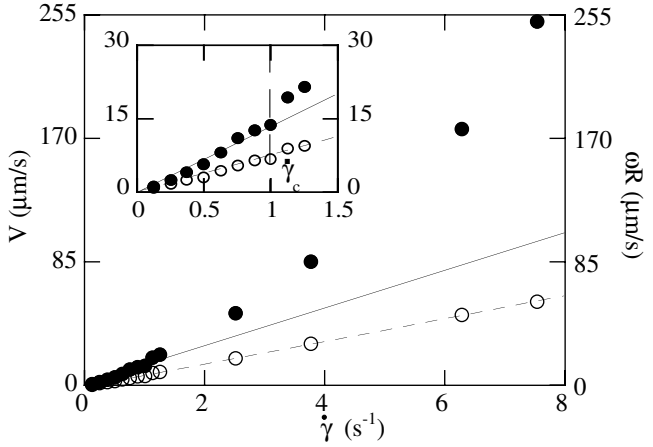

FIG. 2. Translational (V) (•) and rotational (ωR) (∘) velocities versus shear rate $\dot{\gamma}$ ($R = 18$ μm, reduced volume $v = 0.95$, weight $P = 4.2$ pN).

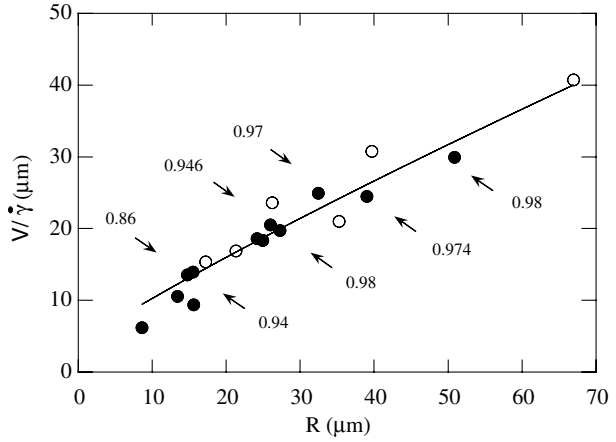

FIG. 3. Variations of the ratio of the velocity to the shear rate $V/\dot{\gamma}$ versus R. Solid line: fit with Goldman's equation [Eq. (1)] with separation distance $h_0 = 2.4\ \mu$m. (∘) deformed vesicles $v < 0.985$ (some reduced volumes are written on the plot); (•) quasispherical vesicles $v \geq 0.985$.

Translational velocity data were fitted using Eq. (1) with one single adjustable parameter h_0. Good agreement is observed, as shown in Fig. 3, yielding $h_0 = 2.4 \pm 0.4\ \mu$m. According to the Goldman model, the ratios $\omega R/V$ of spheres of radius 14.8 and 18 μm, distant at $h_0 = 2.4\ \mu$m from the wall, are equal to 0.485 and 0.50, respectively. These values are in good agreement with the observed values (0.49 and 0.51, respectively) and support the use of this model for vesicles. We will come back to the order of magnitude of h_0 later in this Letter.

Unbinding and lift force.—Nonspherical vesicles unbind when the shear rate exceeds a threshold value $\dot{\gamma}_c$, depending on vesicle weight, radius, and reduced volume. The value $\dot{\gamma}_c$ was determined for each vesicle by two independent methods: first, from the crossover between the two velocity regimes (V versus $\dot{\gamma}$ curves) and, second, from direct measurement of the distance h on side-view images. Both methods yielded the same result. The unbinding phenomenon discloses the existence of a lift force, F_l, acting on nonspherical vesicles, and which is of viscous origin. In the unbound regime, the distance h self-adjusts so that the lift force counterbalances the vesicle weight corrected by the buoyancy of the fluid, $F_l = P = \frac{4\pi R^3}{3}\Delta\rho g$, where $\Delta\rho$ is the density difference between the internal sucrose solution and the external glucose solution of the vesicles and g is the acceleration of gravity. The value of the lift force experienced by a vesicle is therefore known for each detached vesicle. It was found to range from 0.2 to 150 pN, depending on the weight and the reduced volume of the vesicles. Values of $\dot{\gamma}_c$ as small as 0.3 s^{-1} have been observed, for instance, for two vesicles of weight equal to 2.9 and 0.74 pN and reduced volume v equal to 0.94 and 0.98, respectively.

By using dimensional arguments, the lift force can be written as $F_l = \eta\dot{\gamma}R^2\Sigma$, where η is the external fluid viscosity and Σ is a dimensionless function which depends on geometrical parameters: the ratio R/h and the shape of the vesicle. More precisely, the fore-aft curvature difference induced by the flow produces an asymmetric pressure field beneath the vesicle, giving rise to the lift force [2]. Local membrane curvatures are not measured here. Nevertheless, we propose, in a first stage, to account for the deformed shape of vesicles by the global parameter v. A single parameter is sufficient since vesicle shapes are $\dot{\gamma}$ independent in the detached regime. The functional form of the lift force is then expected to be

$$F_l = P = \eta\dot{\gamma}R^2\Sigma\left(\frac{R}{h}, v\right). \tag{2}$$

We explored the R and h dependence and we checked the linear $\dot{\gamma}$ dependence of F_l by analyzing two situations.

At the unbinding transition, the vesicle-substrate distance is a constant, $h = h_0$. The use of vesicles of various weights, radii ($10 < R < 70\ \mu$m), and reduced volumes ($0.86 < v < 0.99$) permitted us to test the $\dot{\gamma}_c$ dependence in a range of one decade ($0.3 < \dot{\gamma}_c < 2.2\ s^{-1}$). We determined the reduced force which, plotted versus $(1 - v)$, yielded a master curve of variations where lie all data points: the best plot was obtained with the reduced variable $F_l/\eta\dot{\gamma}R^3$. In practice, it first appeared, in agreement with Eq. (2), that F_l should be imperatively reduced by $\eta\dot{\gamma}$; the R^3 dependence was set in a second step.

The dependence of the lift force with the distance h was determined beyond unbinding. In this regime, Eq. (2) implies that $\Sigma(h)$ must change like $P/\dot{\gamma}$. For eight vesicles, carefully studied in this regime, h was found to vary linearly with $\dot{\gamma}$ as it clearly appears in Fig. 4. Consequently, the preceding argument imposes that the function Σ must vary with $1/h$ for a detached vesicle.

The lift force therefore writes as

$$F_l = \eta\dot{\gamma}\,\frac{R^3}{h}\,f(1 - v), \tag{3}$$

where $f(1 - v)$ is a dimensionless function of the reduced volume. Finally, we represent in the same plot the variations of $(F_l/\eta R^3)(h/\dot{\gamma})$ versus $(1 - v)$ for vesicles at the unbinding threshold and farther away from the surface (Fig. 5). The ratio $h/\dot{\gamma}$ was determined from the slopes shown in Fig. 4, for the eight vesicles observed far from the wall. For the other vesicles, $h/\dot{\gamma}$ was determined at the unbinding threshold ($\dot{\gamma} = \dot{\gamma}_c$) by adjusting $h = h_0$ in order to superimpose the data to that of the eight previous vesicles. We found $h_0 = 2.4\ \mu$m, which is in good agreement with the value obtained from the previous fit of the curve $V/\dot{\gamma}$ versus R. It supports our hypothesis that the kinematics along the flow direction of deformable vesicles can be described in first approximation with the Goldman model. It strongly suggests that the water film beneath vesicles under shear flow is thick, of the order of a micron. This result differs from that recently reported on quasispherical vesicles either at rest or moving in quiescent fluid ($h_0 \approx 50$ nm) [15,18]. This point has still to be understood.

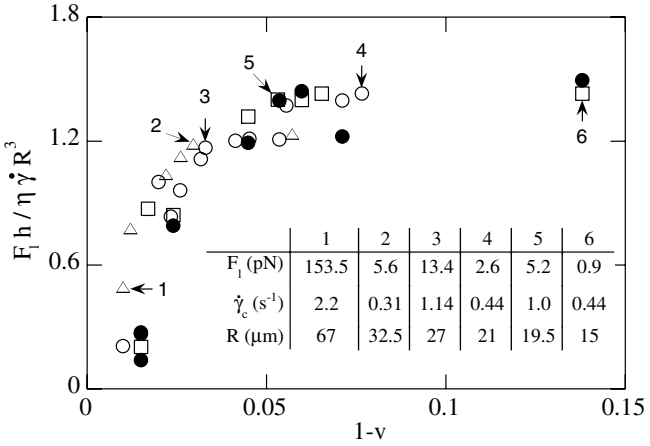

FIG. 5. Variations of $(F_l/\eta R^3)(h/\dot{\gamma})$ versus $(1 - v)$. (Open symbols) vesicles at the unbinding threshold, $\dot{\gamma} = \dot{\gamma}_c$: (□) small radii $R < 20$ μm; (○) intermediate radii $20 \leq R \leq 30$ μm; (△) large radii $R > 30$ μm. (●) Detached vesicles away from the substrate, $\dot{\gamma} > \dot{\gamma}_c$. The three ranges of R are displayed to check the R^3 dependence of the lift force F_l. Some typical values of F_l, $\dot{\gamma}_c$, and R are presented in the table (shown in inset).

Let us briefly discuss Eq. (3). The linear $\dot{\gamma}$ dependence results from the steady tilt of the vesicles observed at unbinding, as clearly explained recently in Ref. [3].

It is worth noting that the R^3/h dependence we found for the lift force is dimensionally consistent. It is valid for vesicles both close to and farther from the wall, in a domain where the lubrication analysis should not hold. The theoretical understanding of this dependence is still an open question. In particular, it cannot be derived by applying the Stokes law in infinite medium to the vertical drift velocity, which would lead to a variation in $R^4/(R + h)^2$, as predicted in Ref. [3].

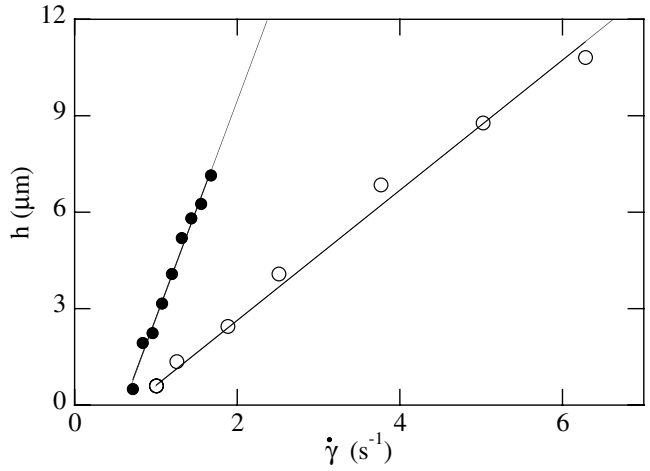

FIG. 4. Variation of distance h to the wall versus the shear rate $\dot{\gamma}$ for two vesicles moving away from the wall. (●) $R = 17$ μm, reduced volume $v = 0.985$, weight $P = 0.2$ pN. (○) $R = 20$ μm, $v = 0.93$, $P = 5.3$ pN.

Concluding remarks.—We described the main features of the behavior of vesicles in a linear shear flow close to a wall: (i) the tank-treading motion; (ii) the lubrication film, which we found thick; (iii) the threshold detachment; (iv) the lift force, whose functional dependence on the relevant parameters was established for detached vesicles. Our results, obtained on vesicles whose inner viscosity is that of the external fluid, should apply to tank-treading cells, such as red blood cells in viscous medium. A further study we hope to report in the near future will explore, on the one hand, the effects of a high contrast viscosity between the inner and the outer fluids and, on the other hand, the effects of attractive interactions between the vesicles and the substrate. These two features are indeed currently observed in living cells.

We thank D. Constantin and J. Beaucourt for experimental help, and Dr. T. Biben and C. Misbah for fruitful discussions and help with the numerical treatment.

*Email address: annie.viallat@ujf-grenoble.fr

[1] U. Seifert, Phys. Rev. Lett. **83**, 876 (1999).
[2] I. Cantat and C. Misbah, Phys. Rev. Lett. **83**, 880 (1999).
[3] S. Sukumaran and U. Seifert, Phys. Rev. E **64**, 011916 (2001).
[4] P. Olla, J. Phys. II (France) **7**, 1533 (1997); Physica (Amsterdam) **278A**, 87 (2000).
[5] S. Torza, R. G. Cox, and S. G. Mason, J. Colloid Interface Sci. **38**, 395 (1972).
[6] T. M. Fischer, M. Stöhr-Liesen, and H. Schmid-Schönbein, Science **202**, 894 (1978).
[7] K-C. Chang, D. F. J. Tees, and D. A. Hammer, Proc. Natl. Acad. Sci. U.S.A. **97**, 11 262 (2000).
[8] O. Tissot, O. A. Pierres, C. Foa, M. Delaage, and P. Bongrand, Biophys. J. **61**, 204 (1992).
[9] B. Lortz, R. Simon, J. Nardi, and E. Sackmann, Europhys. Lett. **51**, 468 (2000).
[10] M. Angelova, S. Soléau, Ph. Méléard, J. F. Faucon, and P. Bothorel, Prog. Colloid Polym. Sci. **89**, 127 (1992).
[11] It is striking to notice that the shapes and orientations of the vesicle observed in Figs. 1(a)–1(d) look very similar to that numerically computed for 2D weakly adhesive vesicles in a bounded linear shear flow (Ref. [2]).
[12] Papus-Guldin theorem on axisymmetric shapes.
[13] M. Kraus, W. Wintz, U. Seifert, and R. Lipowsky, Phys. Rev. Lett. **77**, 3685 (1996).
[14] K. H. de Haas, C. Blom, D. van den Ende, M. H. G. Duits, and J. Mellema, Phys. Rev. E **56**, 7132 (1997).
[15] M. Abkarian, C. Lartigue, and A. Viallat, Phys. Rev. E **63**, 041906 (2001).
[16] T. Biben and C. Misbah (to be published); T. Biben (private communication).
[17] A. J. Goldman, R. G. Cox, and H. Brenner, Chem. Eng. Sci. **22**, 637 (1967).
[18] J. O. Rädler, T. J. Feder, H. H. Strey, and E. Sackmann, Phys. Rev. E **51**, 4526 (1995).